Detection and Characterisation of Faint Transiting Exoplanets TOI 4587 and TOI 5274 using the Bayesian Fitting Tool Juliet

Robin Winterbourne, Evie Cushing, Sergey Najafov, Keisha Shah, Molly Stebbing

July 1, 2026

Abstract

Photometric data from the Transiting Exoplanet Survey Satellite (TESS) was analysed using the Bayesian fitting tool `juliet` to investigate two faint transiting exoplanet targets: the known planet TOI 4587 and the candidate TOI 5274. Models were fitted to all available TESS observations to determine orbital periods, transit geometries and limb-darkening parameters. The derived orbital periods were found to be broadly consistent with published values, although differences between values exceeded quoted uncertainties. TOI 4587 produced a well-constrained solution, while TOI 5274 exhibited broad posterior distributions. Both phase-folded light curves displayed characteristic U-shaped exoplanetary transit signatures. However, the fits performed poorly on the raw photometric data, likely due to the faintness of the targets.

1 Introduction and Theory

Any planet that exists outside of our solar system is known as an exoplanet. Most exoplanets orbit stars, while some float around space without being tethered to any star(Lecavelier des Etangs and Lissauer, 2022). Following the first observed exoplanet to orbit a sun-like star, 51 Pegasi b in 1995, there have been thousands of confirmed exoplanets (Mayor and Queloz, 1995). These discoveries have revealed a diverse range of planetary systems which differ from our own.

Characterising exoplanets helps us understand how other planetary systems form and evolve (Winn and Fabrycky, 2015). By measuring properties such as size, mass, orbital period and composition, researchers can make sense of the diversity of these planetary systems. Moreover, studying exoplanets brings us closer to the search for life somewhere in our universe. However, the first challenge lies in detecting these exoplanets since they are much dimmer than their host stars.

The transit method is one of the most widely used techniques for detecting exoplanets. It is based on measuring small, periodic drops in a star's brightness as a planet passes in front of it along our line of sight (a transit). During a transit a fraction of the star's light is blocked producing a characteristic dip in the observed light curve (Seager and Mallén-Ornelas, 2002). By monitoring the brightness of stars over time, astronomers can identify these repeated dips and infer the presence of an orbiting planet. Additionally, the depth of the transit reveals information about the size of the planet, and the timing between transits gives the orbital period.

The Transiting Exoplanet Survey Satellite (TESS) is a NASA space telescope designed to discover, through the transit method, thousands of exoplanets orbiting the brightest stars in our stellar neighbourhood. TESS operates in an highly elliptical, extremely stable high earth orbit (HEO) with a period of 13.7 days. This HEO maximises the amount of sky that TESS can survey and keeps the spacecraft in a thermally stable, low-radiation environment. The telescopes four wide-field cameras make up, in total, a 24 x 96 degree field of view covering roughly 5% of the sky at any time. Sectors are surveyed for 27 days at a time, with pauses typically at perigee for data downlinks - so every 13.7 days (Ricker *et al.*, 2014).

Robust modelling of TESS's photometric data can be carried out using the Bayesian inference tool Juliet to analyse and characterise planetary systems. A `juliet` light curve model for a given instrument i is given by (Espinoza, Kossakowski, *et al.*, 2019)

$$M_i(t) + \epsilon_i(t), \tag{1}$$

where

$$M_i(t) = [T_i(t)D_i + (1 - D_i)] \left(\frac{1}{1 + D_i M_i} \right), \tag{2}$$

and

$$\epsilon_i(t) \sim \mathcal{N} \left(0, \sqrt{\sigma_i(t)^2 + \sigma_{w,i}^2} \right). \tag{3}$$

The total model (1) is a sum of deterministic physics (the transit and instrument behaviour) $M_i(t)$ and stochastic noise $\epsilon_i(t)$. $T_i(t)$ is the transit model which captures the actual shape of the dip in intensity. It is determined by the planet's size, orbital period, and limb-darkening. D_i is the dilution factor accounting for contaminating light from nearby stars. A dilution factor of one implies no contaminating sources and $D_i < 1$ means that the transit dip would appear shallower due to external light diluting the signal. The final parameter in equation 2 is the relative out-of-transit flux M_i which ensures that the model matches the actual brightness levels of the star when the planet is not transiting. Juliet assumes a default white-Gaussian noise described by equation 3. $\sigma_i(t)$ is the known measurement error at time t and $\sigma_{w,i}$ is an extra term to be fitted. It accounts for 'unknown unknowns' - instrumental noise or stellar activity that the telescope's error bars did not originally capture. The noise is approximately modelled as a normal distribution $\mathcal{N}(\mu, \sigma)$, with a mean of zero and a standard deviation equal to the square root term in equation 3.

Juliet accounts for the fact that stars are not uniformly bright. The centre appears brighter than the edges because light from the limbs come from shallower, cooler layers This is known as limb darkening. A quadratic limb darkening law was assumed relating the intensity at some μ, $I(\mu)$ to the intensity at the centre of the stellar disc $I(1)$ as (Espinoza and Jordán, 2016)

$$\frac{I(\mu)}{I(1)} = 1 - u_1(1 - \mu) - u_2(1 - \mu)^2. \tag{4}$$

$\mu = \cos\theta$, the cosine of the angle θ between the line of sight and the local stellar surface normal. u_1, u_2 are quadratic limb-darkening coefficients,

Rather than fitting the limb-darkening coefficients u_1 and u_2 directly, `juliet` uses the transformed parameters q_1 and q_2 introduced by Kipping (Kipping, 2013). This reparametrisation ensures that the fitted limb darkening coefficients remain physically realistic while improving the efficiency and stability of the fitting process (Claret *et al.*, 2025).

2 Methods

A candidate was systematically selected from ExoFOP (Christiansen *et al.*, 2025) using a tiered filtering system. The first set of filters focused on data quality and availability. It was made sure that TESS picked up at least 3 transits per candidate, with a high SNR and a low TESS magnitude. The second tier of filters regarded stellar characteristics. Stellar type K and M dwarfs are smaller in size and well studied allowing for well-defined priors. Additional parameters like distance from Earth and stellar contamination were considered. The third tier focused on planetary parameters such as radius, period, and impact parameter; selecting bounds on the available data to ensure feasible candidates. The last tier was qualitative - dispositions and comments about the candidates were considered to vet out false positives and select two faint transits, one planet candidate (PC) and one known planet (KP).

All photometric data was obtained from TESS (Ricker *et al.*, 2014). The `lightkurve` (Cardoso *et al.*, 2018) and `juliet` (Espinoza, Kossakowski, *et al.*, 2019; Kreidberg, 2015) libraries were used to access, plot and fit transit models to all available TESS data for the exoplanet candidates. Before fitting, sectors were stitched together and normalised. The Juliet fit used the nested sampler `dynesty` (Speagle, 2020) and phase plots were produced by 'folding' the light curves. Posteriors were obtained and the limb-darkening parameters were compared to theoretical values from ExoCTK's limb-darkening calculator (Bourque *et al.*, 2021).

2.1 Priors

Unless stated otherwise, values to describe the priors (initial assumed probability distributions for each parameter) were taken from published values in the NASA Exoplanet Archive (NASA, n.d.). Distributions were created wider than literature errors to avoid forcing the fit to confirm known precise values.

1. **Orbital Period** (P) - The time taken for a planet to complete one orbit around its host star. Normal distribution.

2. **Mid-Transit Time** (t_0) - The time that relates to the centre of a transit. Used to align the model with the observed light curve. Normal distribution.

3. **Transit Geometry Parameters** (r_1, r_2) - A parametrisation that describes the shape and geometry of the transit. Uniform priors between 0 and 1 were chosen to explore physically valid transit solutions.

4. **Limb-Darkening Parameters** (q_1, q_2) - These are re-parametrised variables that are used to model the limb-darkening. Uniform priors between 0 and 1 were chosen to explore physically valid solutions.

5. **Stellar Density** (ρ_*) - The mean density of the host star. Normal distribution.

6. **Orbital Eccentricity** (e) - Describes how elongated the planetary orbit is. A circular orbit was assumed, fixing the eccentricity to zero.

Other priors (argument of periastron, dilution, flux offset and jitter) were set as the distributions found on Juliet's documentation.

3 Results

Candidate selection revealed two targets of interest (TOIs). A KP (TOI 4587) and a PC (TOI 5274). TOI 4587 is known as Kepler-1624b and orbits a M-dwarf star 259 parsecs away. TOI 5274 was identified in a faint-star search by the quick-look pipeline. The light curve comes from a K-dwarf star 246 parsecs away.

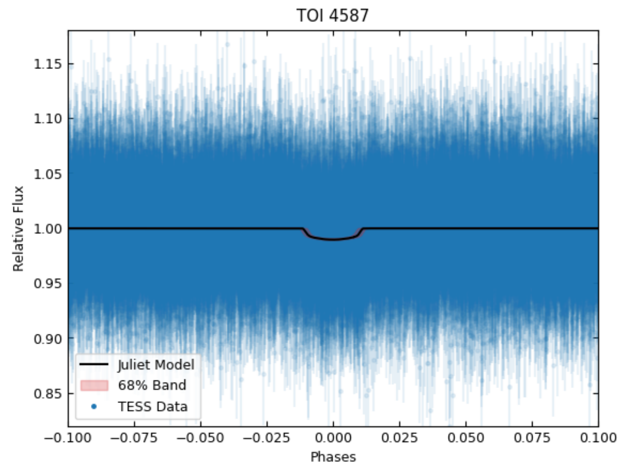

(a) KP

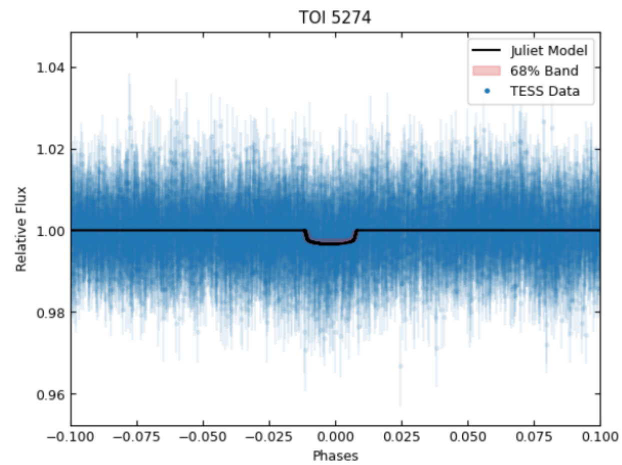

(b) PC

Figure 1: Phase-folded light curves for TOI 4587 (a) and TOI 5274 (b). TESS data is shown in blue. The solid black lines are the Juliet best-fit models with uncertainties shown in red.

Figures 1a and 1b show the phased light curves in blue for both TOIs as well as the `juliet` median models in black with 68% confidence bands in red. Both targets exhibit transit signatures with very faint signals, that are very hard to distinguish visually in the data alone. TOI 4587's transit depth appears much smaller but this is due to the scales of the y-axes. When looking at both y-axes it is clear that the host star of TOI 4587 exhibits much more stellar variability compared to TOI 5274's host star. Relative fluxes range over about 0.2 and 0.04 respectively. Both curves exhibit the flat-bottomed U-shaped dip characteristic of true exoplanet transits.

3.1 TOI 4587

The comprehensive phased light curve for TOI 4587 (figure 1a) displays a well-defined transit profile with the highest uncertainty around the transit edges. The fitting procedure yielded an orbital period of $P = 3.29014728 \pm 0.00000002$ days.

The ratio of the planet radius to the host star radius was determined to be $p = 0.0943 \pm 0.0034$, indicating a gas-giant scale companion. The impact parameter was constrained to $b = 0.46 \pm 0.04$ meaning the orbit had moderate inclination. The effect of this can be seen in the slight curve in the transit (instead of being completely flat-bottomed). No significant correlation was found between the posteriors b and p (figure 5 found in appendix A) confirming a geometrically stable solution for this transit. The derived mean stellar density from the geometric transit parameters was determined to be $\rho_* = 4710^{+80}_{-100}$ kg m^{-3}.

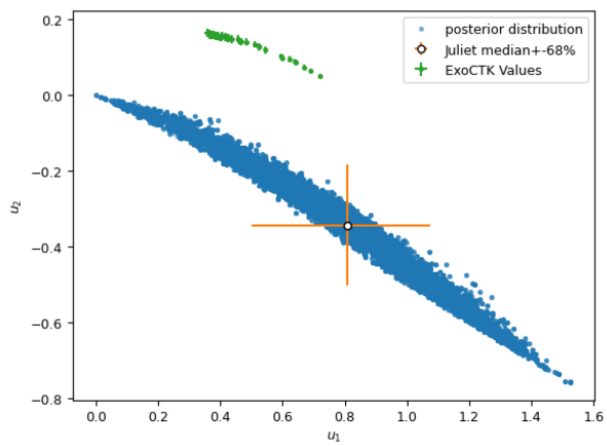

Figure 2: Pairs of limb darkening posteriors in blue for TOI 4587. The median pair is a white circle and uncertainties are shown in orange. Coefficients calculated for TESS's bandpass using ExoCTK are shown in green.

The retrieved quadratic limb-darkening coefficients from the q_1 and q_2 parametrisation converged at $u_1 = 0.81 \pm 0.27$ and $u_2 = -0.35 \pm 0.16$. These median values are plotted along with the full posterior distributions (in blue) in figure 2. ExoCTK values for TESS's bandpass are shown in green. The empirical values demonstrate the same correlation between the limb-darkening coefficients as is seen in the theoretical values, but systematically sit much lower on the y-axis. The median is also skewed to the right compared to ExoCTK.

3.2 TOI 5274

The transit profile for TOI 5274 exhibits a flatter-bottomed U-shaped geometry (figure 1b), representing a more complete transit across the stellar host. The `juliet` fit converged on an orbital period of $P = 6.13997 \pm 0.00004$ days.

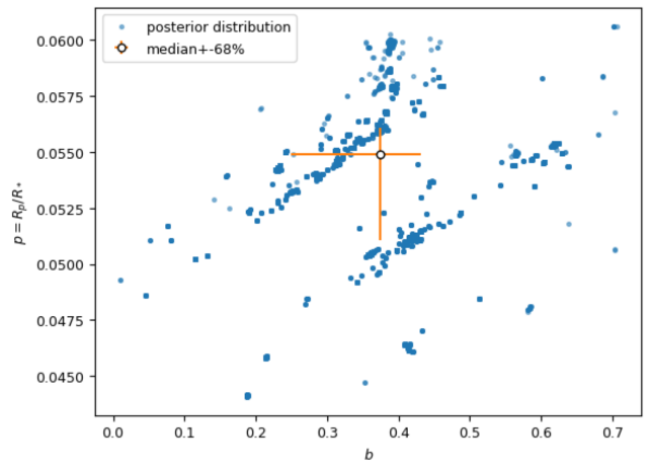

Figure 3: The planet radius to host star ratio p against the impact parameter of the transit b for TOI 5274. Pairs are plotted in blue with the median pair as a white circle. Uncertainties are shown in orange.

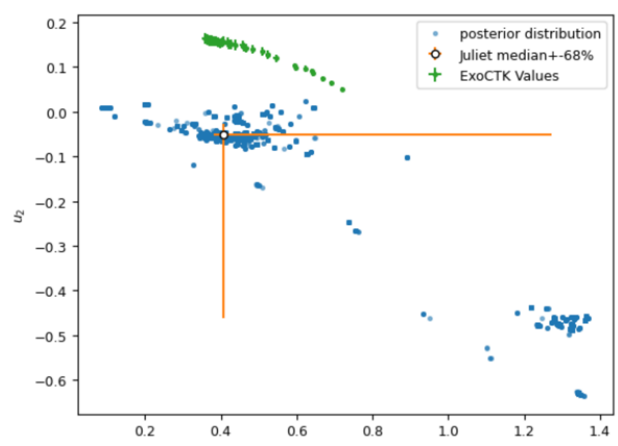

Figure 4: Pairs of limb darkening posteriors in blue for TOI 5274. The median pair is a white circle and uncertainties are shown in orange. Coefficients calculated for TESS's bandpass using ExoCTK are shown in green.

The fitted planet-to-star radius ratio and impact parameter are smaller than that of TOI 4587, yielding $p = 0.0549 \pm 0.0012$ and $b = 0.37^{+0.06}_{-0.13}$. Figure 3 shows high scattering and dual-modal clustering across the parameter space, potentially due to the lower signal-to-noise ratio of this shallow transit. The resulting stellar density was calculated as $\rho_* = 2015^{+9}_{-3}$ kg m^{-3}. Retrieval of the limb-darkening parameters yielded $u_1 = 0.41^{+0.86}_{-0.02}$ and $u_2 = -0.05^{+0.03}_{-0.41}$. As shown in Figure 4, these asymmetric error margins span a wide swath of the parameter space.

4 Discussion

Obtained orbital periods show varying levels of agreement with literature values. For TOI 4587, the derived period of $P = 3.29014728 \pm 0.00000002$ days differs from the published value of 3.2903041 ± 0.00001 days by only $\tilde{1}3.5$ s, excellently agreeing. However, this discrepancy is larger than the combined quoted uncertainties. For TOI 5274, $P = 6.13997 \pm 0.00004$ days deviates from the literature value of 6.13135 ± 0.00003days by 12.4 min. This only represents 0.14% of the orbital period. But similarly to TOI 4587, it is substantially larger than the associated uncertainties. Therefore, for both candidates, as the discrepancies are unlikely to arise from random error alone, errors may be underestimated or the differences may reflect the data quality or fitting methodology.

Whilst the symmetric flat-bottomed profiles of the two phased transits match the expected signatures of clean exoplanetary transits, the raw light curves (figure 6 found in appendix B) look visually strange. The fit predicts transits where almost no decrease in intensity can be seen and seems inconsistent in what it determines as a transit and what as noise. This could indicate problems with the fit, where the convincing phase-folded transit profiles may be an artefact of the fitting procedure rather than a valid detection from the raw data. Future work should assess the robustness of these detections by acquiring additional photometric data or fitting to data from other instruments. Consistent transit depths and durations across multiple instruments and observations would confirm that these signals are genuine. Furthermore, transits may not occur at perfectly rigid intervals. Accounting for non-Keplerian variations by including transit timing variations (TTVs) in the `juliet` fit could improve the fits greatly.

The clear convergence of the TOI 4587's limb-darkening coefficients (u_1, u_2) and their tight agreement with the ExoCTK model confirm that the host star behaves as standard. The lack of correlation between the impact parameter b and radius ratio p points to a highly reliable physical solution. In contrast, TOI 5274's parameters are less secure. The small radius ratio ($p = 0.0549 \pm 0.0012$) produces a shallow transit that increases the scatter in the joint posteriors. This lower signal-to-noise ratio explains why the b vs. p distribution displays a stretched, dual-modal shape. Furthermore, the limb-darkening parameters u_1 and u_2 are highly unconstrained and deviate significantly from the theoretical green curves in Figure 4. This structural mismatch suggests that the single-planet model might be struggling with the faint signal or a diluted background light source. This is corroborated by looking at the target pixel file data which reveals a possible slight movement of the target star image cluster near frame 1920. A centroid-shift analysis on the pixel frames is needed to ensure the signal is not contaminated by a nearby star or background binary. Overall, the poorly constrained b-p and u_1-u_2 posterior distributions indicate that the data cannot uniquely constrain these parameters. Degeneracies allow different combinations of impact parameter, planet radius ratio and limb-darkening coefficients to produce similarly good fits to the transit.

Future work could seek to confirm these candidates using radial velocity observations. While the transit method primarily constrains planetary radius and orbital properties, radial velocity measurements can provide estimates of planetary mass through detection of the host star's Doppler-induced motion (Fischer *et al.*, 2016). Joint-fits (transit and radial velocity) would determine planets' densities, helping to distinguish between rocky planets and gas giants (Seager and Mallén-Ornelas, 2002).

5 Conclusions

TESS photometry and the Bayesian fitting package `juliet` were used to detect and characterise two transiting exoplanet targets, TOI 4587 and TOI 5274. Transit models were successfully fitted to both systems, producing estimates for orbital periods, transit geometries and limb-darkening parameters. The derived orbital periods show general agreement with published values, although errors are likely underestimated.

The results indicate that TOI 4587 is the more robustly constrained system. Its transit geometry is well defined, and the limb-darkening coefficients broadly follow theoretical trends. In contrast, TOI 5274's poorly constrained b-p and u_1-u_2 parameter spaces suggest that the fit is unable to uniquely determine the transit geometry and limb-darkening profile, likely due to the shallow transit signal.

Although the phase-folded light curves display convincing transit signatures, the weakness of the plots over the raw data means that the results should be treated with caution. Additional photometric observations, TTV fitting, centroid analysis and radial velocity follow-up would help verify or challenge the planetary nature of these signals and improve constraints on their physical properties.

References

Bourque, M. *et al.* (2021). *The Exoplanet Characterization Toolkit (ExoCTK).*

Cardoso, J. V. d. M. *et al.* (2018). *Lightkurve: Kepler and TESS time series analysis in Python.*

Christiansen, J. L. *et al.* (2025). "The NASA Exoplanet Archive and Exoplanet Follow-up Observing Program: Data, Tools, and Usage". *Planetary Science Journal* 6.8.

Claret, A., P. H. Hauschildt, and G. Torres (2025). "Limb-Darkening Coefficients for the 4-Term and Power-2 Laws for the JWST Space Mission, Adopting PHOENIX Spherical Models at High Resolution".

Espinoza, N. and A. Jordán (2016). "Limb darkening and exoplanets - II. Choosing the best law for optimal retrieval of transit parameters". *Monthly Notices of the Royal Astronomical Society* 457.4, pp. 3573–3581.

Espinoza, N., D. Kossakowski, and R. Brahm (2019). "Juliet: a versatile modelling tool for transiting and non-transiting exoplanetary systems".

Fischer, D. *et al.* (2016). "State of the Field: Extreme Precision Radial Velocities".

Kipping, D. M. (2013). "Efficient, uninformative sampling of limb darkening coefficients for two-parameter laws". *Monthly Notices of the Royal Astronomical Society* 435.3, pp. 2152–2160.

Kreidberg, L. (2015). *batman: BAsic Transit Model cAlculatioN in Python.* Tech. rep.

Lecavelier des Etangs, A. and J. J. Lissauer (2022). "The IAU working definition of an exoplanet". *New Astronomy Reviews* 94, p. 101641.

Mayor, M. and D. Queloz (1995). "A Jupiter-mass companion to a solar-type star". *Nature* 378.

NASA (n.d.). *KOI-5274 Overview.*

Ricker, G. R. *et al.* (2014). "The Transiting Exoplanet Survey Satellite". *Journal of Astronomical Telescopes, Instruments, and Systems.*

Seager, S. and G. Mallén-Ornelas (2002). *A Unique Solution of Planet and Star Parameters from an Extrasolar Planet Light Curve.* Tech. rep.

Speagle, J. S. (2020). "DYNESTY: a dynamic nested sampling package for estimating Bayesian posteriors and evidences". *Monthly Notices of the Royal Astronomical Society* 493.3, pp. 3132–3158.

Winn, J. N. and D. C. Fabrycky (2015). *The occurrence and architecture of exoplanetary systems.*

A TOI 4587 b-p Plot

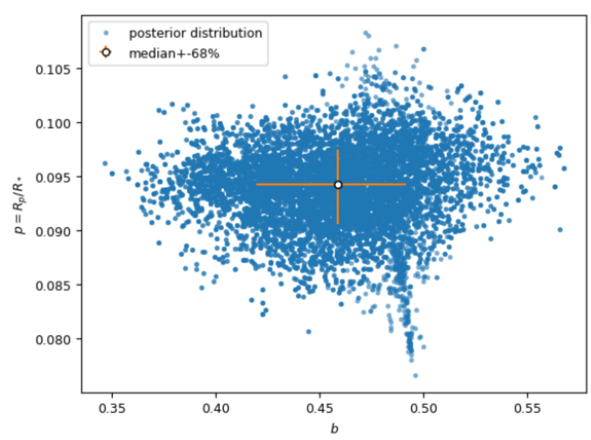

Figure 5: The planet radius to host star ratio p against the impact parameter of the transit b for TOI 4587. Pairs are plotted in blue with the median pair as a white circle. Uncertainties are shown in orange.

B Full Light Curves

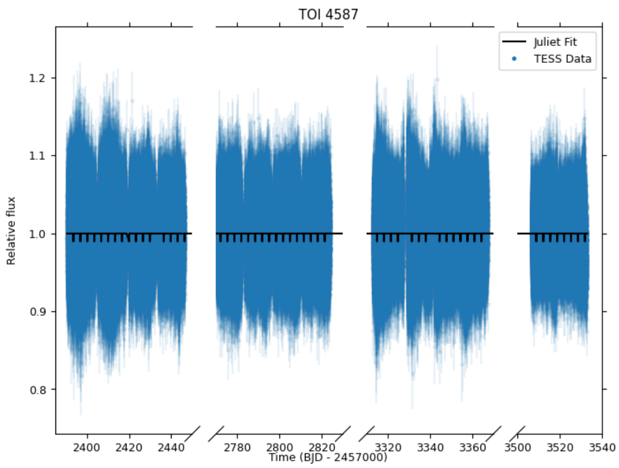

(a) KP

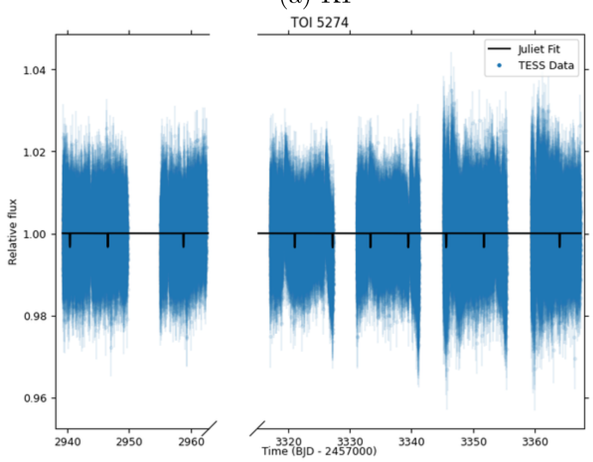

(b) PC

Figure 6: TESS photometric data from all available searches is shown in blue for TOI 4587 (a) and TOI 5274 (b). The `juliet` fits are shown in black.